Supporting Information (SI)

A dioxadithiaazacrown ether-BODIPY dyad Hg^{2+} complex for detection of L-cysteine: Fluorescence switching and application on soft material

Navdeep Kaur, Paramjit Kaur* and Kamaljit Singh*

Department of Chemistry, UGC-Centre of Advanced Studies-I, Guru Nanak Dev University, Amritsar-143 005, Punjab, India.
E-mail: paramjit19in@yahoo.co.in; kamaljit.chem@gndu.ac.in

Table of Contents

General note to physical measurements:

^{1}H NMR (300 MHz) spectra were recorded in CD_3CN on a JEOL-FT NMR-AL. Tetramethylsilane (TMS) served as the internal standard (0 ppm for ^{1}H). Mass spectra were recorded on a Bruker micrOTOF-Q II 10356 spectrometer. Emission studies were made on Perkin Elmer LS 55 Fluorescence Spectrometer with excitation slit width as 10.0 and emission slit width as 5 with off emission correction mode. UV-Vis spectra were recorded on a HITACHI U-2900 spectrophotometer, with a quartz cuvette (path length, 1 cm) and studies were performed in AR grade acetonitrile. The cell holder of the spectrophotometer was maintained at 25^0C (Peltier) for consistency in the recordings.

Quantum yield calculations:

The fluorescence quantum yields were measured with respect to 9, 10-diphenylanthracene as standard having quantum yield of 0.86 in cyclohexane.[1]

$\Phi_u = \Phi_s \cdot F_u.A_s.\eta_u^2 / F_s.A_u.\eta_s^2$

Φ = quantum yield

F = Integrated fluorescence intensity

A = Absorbance

η = refractive index of solvent

s = standard i.e. 9, 10-diphenylanthracene

u = sample

Detection limit calculations:

The detection limit was calculated on the basis of the fluorescence titration. The fluorescence emission measurement of **2** was repeated 6 times, to deduce standard deviation (σ) of blank measurement. To calculate the slope (K), ratio of the emission intensity at 520 nm was plotted against the concentration of cys. The detection limit was calculated using the following equation.

$$\text{Detection limit} = 3 \times \sigma / K$$

Computational details:

All theoretical calculations were carried out by using the Gaussian 09 suite of programs.[2] The molecular geometries of the chromophores were optimized at the DFT method employing the hybrid MPW1PW91 functional. The 6-31G* basis set was used for C, H, B, F, Cl, N, S, and O atoms

whereas SDD with effective core potential for the metal ions was used for Hg^{2+}. The molecular structure was plotted using Gauss view 5.0.9.

Studies on the detection of Hg^{2+} by 1:

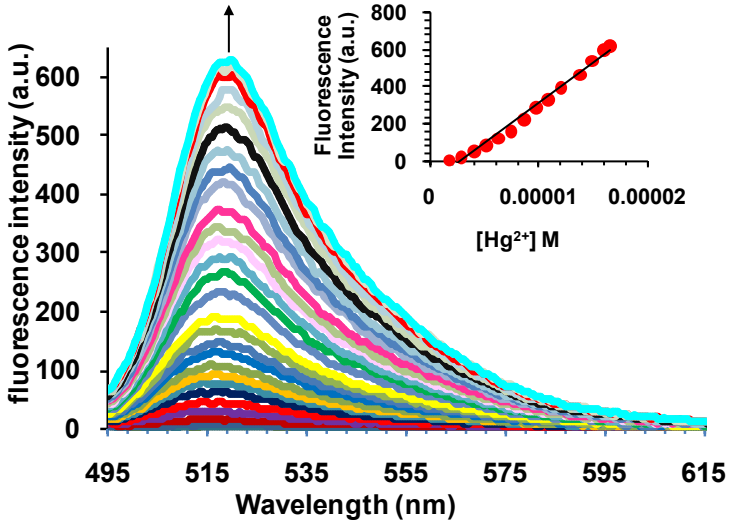

Fig. S1 Changes in the emission spectrum of **1** (5 x 10^{-6} M, in CH_3CN) upon addition of different concentrations of Hg^{2+} (2.87 x 10^{-7} M to 1.14 x 10^{-5} M in water) in CH_3CN.

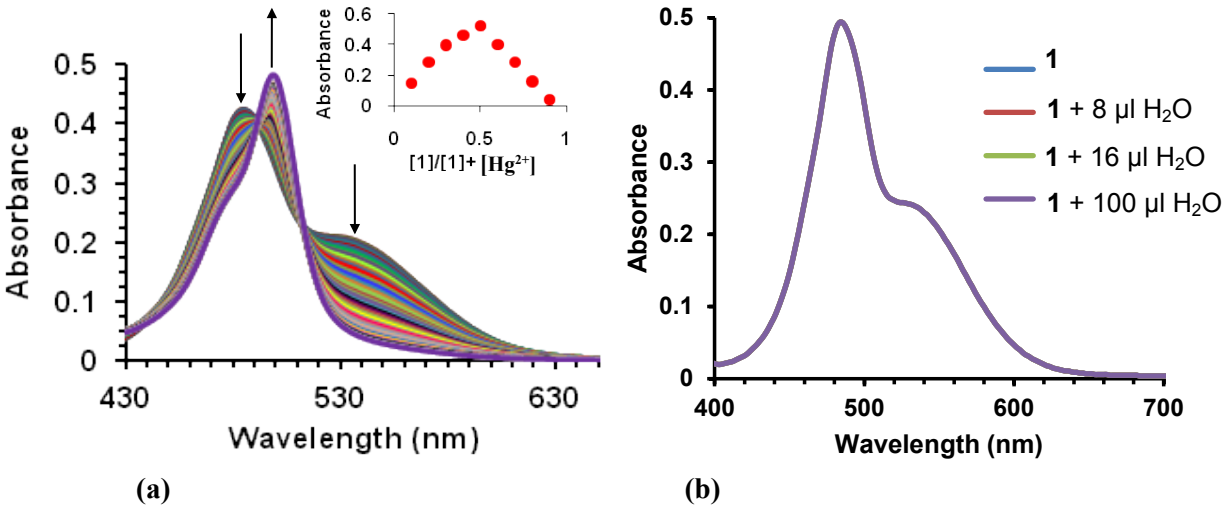

Fig. S2 (a) Changes in the absorption spectrum of **1** (1 x 10^{-5} M, in CH_3CN) upon addition of different concentrations of Hg^{2+} (2.85 x 10^{-7} to 2.28 x 10^{-5} M in water), in CH_3CN. (b) Changes in the absorption spectrum of **1** (1 x 10^{-5} M, in CH_3CN) upon addition of different amounts of H_2O.

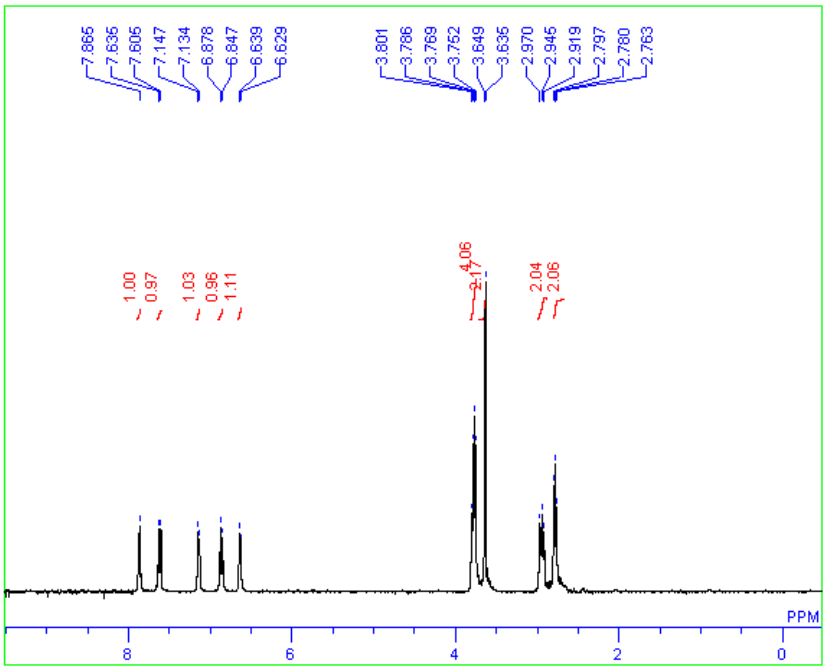

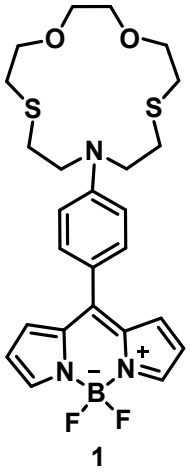

1

Fig. S3 ^{1}H NMR of **1** in CD_3CN.

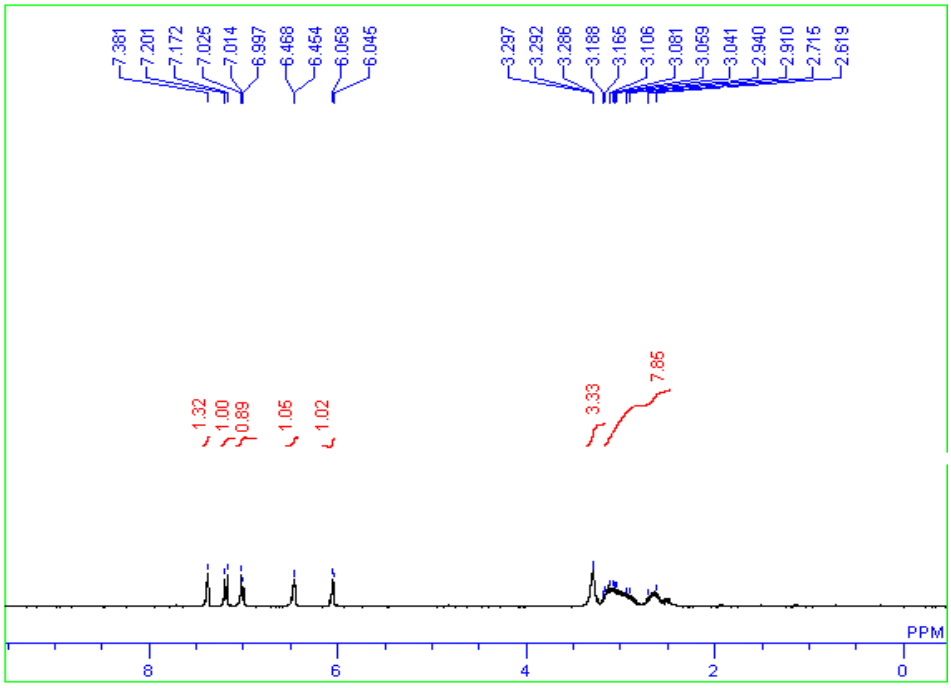

Fig. S4 ^{1}H NMR of **1**:Hg^{2+}(**2**) complex (**1** and Hg^{2+} in CD_3CN).

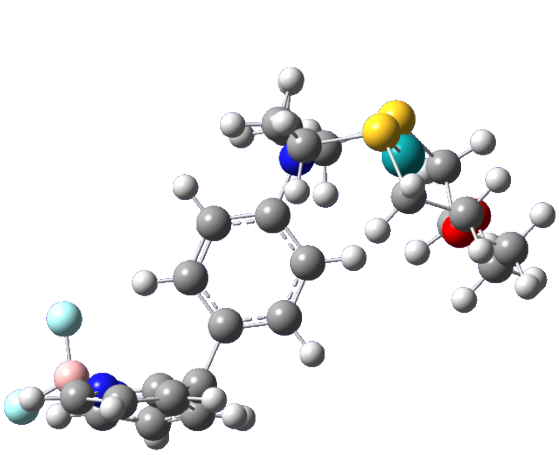

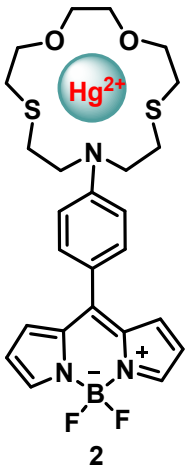

Fig. S5 Optimized structure of **2** (color notation in the structure is as follows: Grey-Carbon, White-Hydrogen, Yellow-Sulphur, Dark blue-Nitrogen, Sky blue-Flourine, Red-Oxygen, Green-Mercury, Pink-Boron)**.**

Table S1: Cartesian coordinates of **2.**

Center Number	Atomic Number	Coordinates (Angstroms) X	Y	Z
1	6	-1.495074	-0.045411	-1.617078
2	6	-0.259175	-0.000889	-0.958797
3	6	-0.236380	0.069008	0.429645
4	6	-1.428165	0.090943	1.158031
5	6	-2.657691	0.041489	0.505242
6	6	-2.677139	-0.028214	-0.895745
7	1	-1.547870	-0.093617	-2.701164
8	1	0.711554	0.121261	0.965359
9	1	-1.390473	0.148768	2.241409
10	1	-3.626833	-0.069685	-1.423292
11	7	0.982333	-0.008875	-1.725834
12	1	1.866119	-1.058228	-3.324432
13	1	0.242136	1.386450	-3.154798
14	6	1.576977	-2.440601	-1.689066

15	6	1.357409	2.469235	-1.712810
16	6	1.139050	-1.242664	-2.527493
17	6	1.137590	1.211521	-2.546225
18	1	0.194957	-1.508594	-3.014466
19	1	1.972469	1.065339	-3.238641
20	1	1.489287	-3.357290	-2.276687
21	1	1.311041	3.347705	-2.359684
22	1	0.595507	2.562916	-0.935083
23	1	0.967642	-2.534556	-0.786722
24	16	3.351126	-2.264916	-1.243392
25	16	3.017386	2.506436	-0.910828
26	6	3.583993	-3.298747	0.245595
27	6	2.685265	3.261325	0.732118
28	1	4.668958	-3.414558	0.312930
29	1	1.622426	3.144137	0.954705
30	6	3.028300	-2.732494	1.538996
31	6	3.526803	2.629553	1.823702
32	1	3.375451	-3.373396	2.358172
33	1	1.930385	-2.726551	1.552849
34	1	4.600889	2.712309	1.613055
35	1	3.320094	3.162229	2.759543
36	8	3.531848	-1.418327	1.706694
37	8	3.145701	1.268448	1.952594
38	6	3.301902	-0.850705	2.994438
39	6	3.843298	0.556094	2.973572
40	1	2.228196	-0.851167	3.218936
41	1	3.824590	-1.436588	3.758297

42	1	4.919394	0.556837	2.762490
43	1	3.671183	1.030924	3.945691
44	6	-3.976869	0.062779	1.293534
45	1	-3.719608	0.143512	2.357666
46	6	-4.591339	2.618634	1.292497
47	6	-6.405481	2.405546	-0.007623
48	6	-5.634975	3.331491	0.713724
49	1	-3.815251	2.999614	1.941291
50	1	-7.303246	2.551617	-0.589912
51	1	-5.844426	4.386438	0.809758
52	6	-4.452705	-2.498351	1.644656
53	6	-5.453540	-3.339411	1.171585
54	1	-3.660376	-2.744560	2.337472
55	6	-6.269075	-2.564366	0.331945
56	1	-5.606344	-4.381011	1.411822
57	1	-7.155050	-2.837110	-0.222175
58	6	-4.701515	-1.224736	1.090643
59	6	-4.769642	1.269201	0.919495
60	7	-5.796666	-1.291934	0.290220
61	7	-5.864795	1.166732	0.123112
62	5	-6.315882	-0.132100	-0.615120
63	9	-7.670719	-0.178060	-0.743855
64	9	-5.656277	-0.196022	-1.844391
65	1	2.919605	4.324514	0.645329
66	1	3.154604	-4.281149	0.032115
67	80	3.050147	0.060282	-0.30785

Determination of binding constant:

Binding constant was determined from the slope of the plot Xo-X/X-X_{lim} vs [cys], where Xo = absorbance of sensor **2** without cys; X = absorbance of **2**+cys after each addition; X_{lim} = absorbance of titration solution at very high concentration of cys.

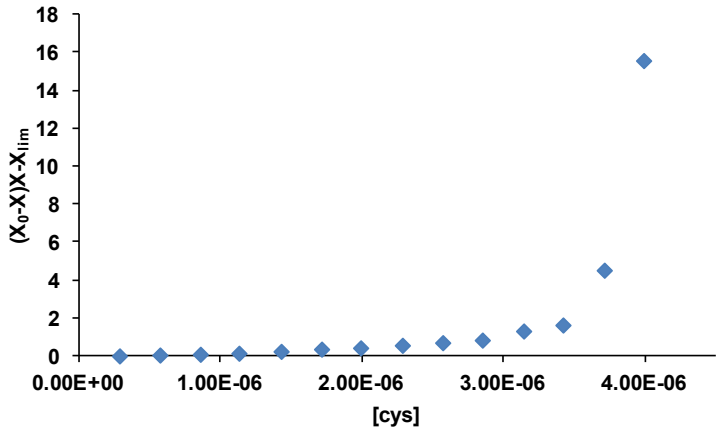

Fig. S6 Plot of Xo-X/X-X_{lim} vs [cys] for determination of binding constants.

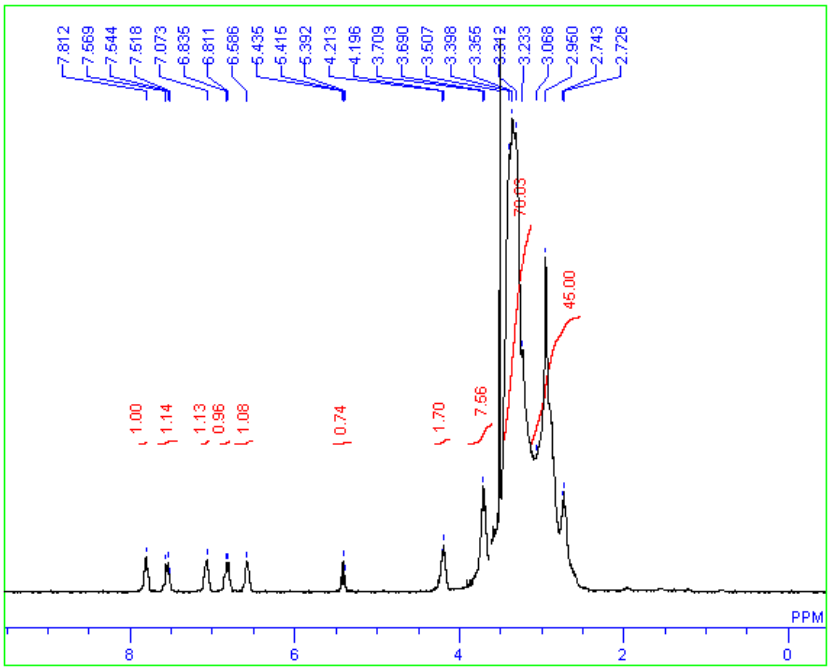

Fig. S7 ^{1}H NMR of **2**+cys (**1** and Hg^{2+} in CD_3CN and cys in D_2O)

Table. S2 Representative detection limits for cys reported by various research groups

S. No.	Detection Limit	Reference
1	3.9 nM	3
2	10μM	4
3	0.46μM	5
4	0.08μM	6
5	19nM	7
6	0.008μM	8
7	5nM	9
8	0.18μM	10
9	2.7μM	11
10	0.28μM	12
11	0.03μM	13
12	10^{-5}M	14
13	0.22μM	15
14	91.3nM	16

References:

1. J. V. Morris, M. A. Mahaney and J. R. Huber, *J. Phys. Chem. B*., 1976, **80**, 969.
2. Gaussian 09, Revision B.01, M. J. Frisch, G. W. Trucks, H. B. Schlegel, G. E. Scuseria, M. A. Robb, J. R. Cheeseman, G. Scalmani, V. Barone, B. Mennucci, G. A. Petersson, H. Nakatsuji, M. Caricato, X. Li, H. P. Hratchian, A. F. Izmaylov, J. Bloino, G. Zheng, J. L. Sonnenberg, M. Hada, M. Ehara, K. Toyota, R. Fukuda, J. Hasegawa, M. Ishida, T. Nakajima, Y. Honda, O. Kitao, H. Nakai, T. Vreven, J. A. Montgomery, Jr., J. E. Peralta, F. Ogliaro, M. Bearpark, J. J. Heyd, E. Brothers, K. N. Kudin, V. N. Staroverov, T. Keith, R. Kobayashi, J. Normand, K. Raghavachari, A. Rendell, J. C. Burant, S. S. Iyengar, J. Tomasi, M. Cossi, N. Rega, J. M. Millam, M. Klene, J. E. Knox, J. B. Cross, V. Bakken, C. Adamo, J. Jaramillo, R. Gomperts, R. E. Stratmann, O. Yazyev, A. J. Austin, R. Cammi, C. Pomelli, J. W. Ochterski, R. L. Martin, K. Morokuma, V. G. Zakrzewski, G. A. Voth, P. Salvador, J. J. Dannenberg, S. Dapprich, A. D. Daniels, O. Farkas, J. B. Foresman, J. V. Ortiz, J. Cioslowski, and D. J. Fox, Gaussian, Inc., Wallingford CT, **2010**.
3. Z.Yan, S. Guang, H. Xu and X. Liu*, Analyst*, 2011, **136**, 1916.
4. X. Wei, L. Qi, J. Tan, R. Liu and F. Wang, *Anal. Chim. Acta*, 2010, **671**, 80–84.
5. H. Razmi and H. Heidari, *Anal. Biochem*., 2009, **388**, 15‑22.
6. L. P. Liu, Z. J. Yin and Z. S. Yang, *Bioelectrochemistry*, 2010, **79**, 84–89.

7. S. M. Jia, X. F. Liu, P. Li, D. M. Kong and H. X. Shen, *Biosens. Bioelectrons.,* 2011, **27** 148–152.

8. H. Hosseini, H. Ahmar, A. Dehghani, A. Bagheri, A. Tadjarodi and A. R. Fakhari, *Biosens. Bioelectrons.,* 2013, **42**, 426–429.

9. H. Su, F. Qiao, R. Duan, L.Chen and S. Ai, *Biosens. Bioelectrons.,* 2013, **43**, 268–273.

10. P. C. Pandey, A. K. Pandey and D. S. Chauhan, *Electrochimica Acta*, 2012, **74**, 23– 31.

11. M. Santhiago, P. R. Lima, W. de. J. R. Santos and L. T. Kubota, *Sens. Actuators B,* 2010, **146** 213–220.

12. H. Yan, H. Su, D. Tian, F. Miao and H. Li, *Sens. Actuators B,* 2011, **160**, 656– 661.

13. J. M. Liu, L. Jiao, L. H. Zhang, Z. Y. Zheng, X. X. Wang, L. P. Lin and S. L. Jiang, *Sens. Actuators B,* 2013, **188,** 613– 620.

14. P. D. Torre, O. G. Beltrán, W. Tiznado, N. Mena, L. A. Saavedra, M. G. Cabrera, J. Trilleras, P. Pavez and M. E. Aliaga, *Sens. Actuators B,* 2014, **193**, 391– 399.

15. F. Miao, J. Zhan, Z. Zou, D. Tian and H. Li, *Tetrahedron,* 2012 **68** 2409-2413.

16. H. P. Fang, M. Shellaiah, A. Singh, M. V. R. Raju, Y. H. Wu and H. C. Lin, *Sens. Actuators B,* 2014, **194**, 229– 237.